

**Supporting Information for:**

**Rotational Spectrum of Laser-Ablated Mannitol: A Conformational and Photofragmentation Study**

S. Mato,<sup>a</sup> E. R.Alonso,<sup>a</sup> E. Martínez-Núñez,<sup>b</sup> A. Fernández-Ramos,<sup>bc</sup> I.León,<sup>a</sup> S.Mata,<sup>a</sup> J. L. Alonso<sup>\*a</sup>

---

<sup>a</sup> Grupo de Espectroscopia Molecular (GEM), Edificio Quifima, Laboratorios de Espectroscopia y Bioespectroscopia, Parque Científico UVa, Universidad de Valladolid, 47011, Valladolid, Spain.

<sup>b</sup> Departamento de Química Física, Facultad de Química, Universidade de Santiago de Compostela, Avda. das Ciencias s/n 15782, Santiago de Compostela, España

<sup>c</sup> Centro Singular de Investigación en Química Biológica y Materiales Moleculares (CIQUS), Universidade de Santiago de Compostela, C/Jenaro de la Fuente s/n, Santiago de Compostela, España

**Figure S01:** LA-CP-FTMW spectrum of mannitol: (a) 2-8 GHz and (b) 6-12 GHz.

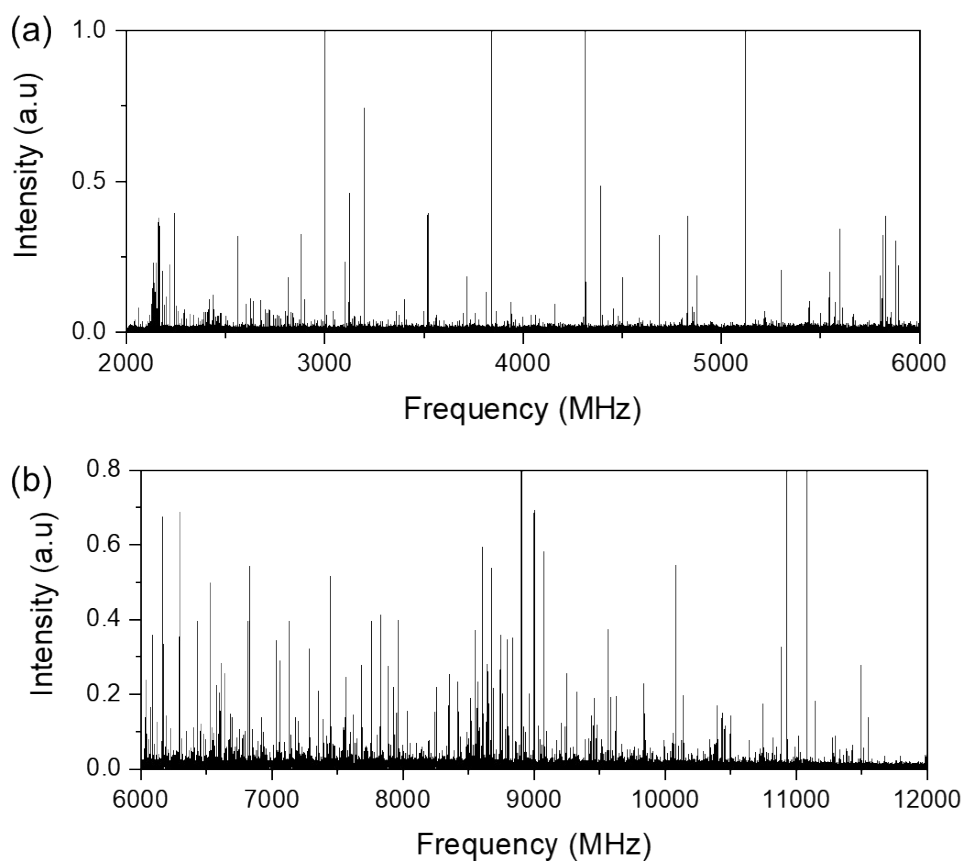


**Table S01.** Predicted parameters for mannitol conformers at different computational methodologies.

TG+T/G+G+c	B3LYP-GD3BJ	MP2	B2PLYPD	TG+T/G+T/c	B3LYP-GD3BJ	MP2	B2PLYPD
A	1662	1679	1672	A	1668	1669	1670
B	537	547	541	B	517	524	519
C	444	452	447	C	418	424	420
$\mu_a$	-0.3	0.1	0.2	$\mu_a$	2.5	2.6	2.6
$\mu_b$	-0.4	0.4	0.4	$\mu_b$	0.2	-0.2	-0.2
$\mu_c$	0.3	0.3	0.3	$\mu_c$	-0.9	0.9	0.9
$\Delta E$	16	0	0	$\Delta E$	182	160	127
$\Delta E_{ZPE}$	0	0	0	$\Delta E_{ZPE}$	119	118	85
$\Delta G_{298K}$	0	0	0	$\Delta G_{298K}$	244	143	177

TG-T/TT/c	B3LYP-GD3BJ	MP2	B2PLYPD	TG+T/G+T/c'	B3LYP-GD3BJ	MP2	B2PLYPD
A	1491	1477	1488	A	1670	1670	1672
B	489	496	492	B	514	521	516
C	475	486	479	C	416	422	418
$\mu_a$	0.0	0.0	0.0	$\mu_a$	1.4	1.4	1.4
$\mu_b$	0.0	0.0	0.0	$\mu_b$	0.3	-0.3	-0.3
$\mu_c$	-1.4	-1.4	-1.4	$\mu_c$	0.9	-0.9	-0.9
$\Delta E$	575	640	561	$\Delta E$	199	290	191
$\Delta E_{ZPE}$	330	367	315	$\Delta E_{ZPE}$	163	239	161

$\Delta G_{298K}$	356	291	309	$\Delta G_{298K}$	299	252	257
TG-T/TT/c'	B3LYP-GD3BJ	MP2	B2PLYPD	TG+T/G+G+/c	B3LYP-GD3BJ	MP2	B2PLYPD
A	1499	1483	1495	A	1618	1637	1626
B	486	494	489	B	542	549	545
C	472	484	476	C	448	454	450
$\mu_a$	1.7	1.8	1.8	$\mu_a$	-2.8	2.8	2.8
$\mu_b$	-0.7	-0.7	-0.7	$\mu_b$	0.5	-0.6	-0.5
$\mu_c$	-2.4	-2.4	-2.4	$\mu_c$	0.4	0.4	0.4
$\Delta E$	609	767	636	$\Delta E$	295	306	266
$\Delta E_{ZPE}$	400	524	422	$\Delta E_{ZPE}$	265	281	250
$\Delta G_{298K}$	447	466	433	$\Delta G_{298K}$	395	288	343
TTG-/G-T/c	B3LYP-GD3BJ	MP2	B2PLYPD	TG-T/TG+/c	B3LYP-GD3BJ	MP2	B2PLYPD
A	1484	1486	1487	A	1701	1690	1699
B	524	529	526	B	496	504	499
C	458	465	461	C	459	470	463
$\mu_a$	3.9	3.9	3.9	$\mu_a$	2.1	2.2	2.1
$\mu_b$	-1.9	-2.0	-1.9	$\mu_b$	-0.7	-0.8	-0.7
$\mu_c$	-0.2	-0.2	-0.2	$\mu_c$	-0.3	-0.3	-0.3
$\Delta E$	406	445	406	$\Delta E$	508	778	599
$\Delta E_{ZPE}$	363	427	385	$\Delta E_{ZPE}$	371	580	450
$\Delta G_{298K}$	518	498	517	$\Delta G_{298K}$	409	464	339
G-TG-/TT/c	B3LYP-GD3BJ	MP2	B2PLYPD	TG-T/TT/c''	B3LYP-GD3BJ	MP2	B2PLYPD
A	1775	1780	1778	A	1509	1491	1504
B	463	468	465	B	484	491	486
C	437	442	439	C	469	481	474
$\mu_a$	0.0	0.0	0.0	$\mu_a$	0.0	0.0	0.0
$\mu_b$	1.0	1.0	-1.0	$\mu_b$	0.0	0.0	0.0
$\mu_c$	0.0	0.0	0.0	$\mu_c$	-3.4	-3.4	-3.4
$\Delta E$	196	431	316	$\Delta E$	661	915	729
$\Delta E_{ZPE}$	163	395	291	$\Delta E_{ZPE}$	487	696	545
$\Delta G_{298K}$	360	478	449	$\Delta G_{298K}$	552	652	573
G-TG-/G+T/c	B3LYP-GD3BJ	MP2	B2PLYPD	TG-T/G+T/c	B3LYP-GD3BJ	MP2	B2PLYPD
A	1565	1588	1573	A	1701	1689	1698
B	529	533	530	B	499	508	503
C	497	504	499	C	462	474	467
$\mu_a$	-2.0	-2.0	2.0	$\mu_a$	-0.2	-0.2	-0.2
$\mu_b$	0.9	0.7	-0.8	$\mu_b$	0.5	0.5	0.5
$\mu_c$	-0.7	-0.7	-0.7	$\mu_c$	-1.6	-1.8	-1.7
$\Delta E$	303	539	418	$\Delta E$	724	866	757
$\Delta E_{ZPE}$	246	442	356	$\Delta E_{ZPE}$	561	671	590
$\Delta G_{298K}$	456	518	519	$\Delta G_{298K}$	633	632	625
TTG+/TG-/cc	B3LYP-GD3BJ	MP2	B2PLYPD	G-TG-/G+G+/c	B3LYP-GD3BJ	MP2	B2PLYPD

A	1626	1634	1630	A	1417	1445	1427
B	498	504	500	B	593	595	594
C	437	442	439	C	581	588	583
$\mu_a$	0.5	-0.4	-0.5	$\mu_a$	0.0	0.0	0.0
$\mu_b$	-0.1	0.2	0.1	$\mu_b$	0.2	0.1	-0.1
$\mu_c$	0.3	0.3	0.3	$\mu_c$	0.0	0.0	0.0
$\Delta E$	877	1054	908	$\Delta E$	393	671	517
$\Delta E_{ZPE}$	664	811	693	$\Delta E_{ZPE}$	336	528	439
$\Delta G_{298K}$	763	773	744	$\Delta G_{298K}$	576	630	631
G+G+T/TG+/c	B3LYP-GD3BJ	MP2	B2PLYPD	G-TG-/G-T/c	B3LYP-GD3BJ	MP2	B2PLYPD
A	1427	1423	1426	A	1407	1412	1409
B	551	562	555	B	564	573	567
C	453	461	456	C	488	495	490
$\mu_a$	-0.3	0.1	0.2	$\mu_a$	-2.4	2.5	2.5
$\mu_b$	-0.3	-0.2	-0.3	$\mu_b$	-0.5	0.6	0.6
$\mu_c$	-0.4	0.4	0.4	$\mu_c$	0.8	0.9	0.8
$\Delta E$	838	786	808	$\Delta E$	573	640	619
$\Delta E_{ZPE}$	700	659	677	$\Delta E_{ZPE}$	511	573	564
$\Delta G_{298K}$	723	635	681	$\Delta G_{298K}$	675	642	695
G+TG-/TT/cc	B3LYP-GD3BJ	MP2	B2PLYPD	TG+T/TG-/c	B3LYP-GD3BJ	MP2	B2PLYPD
A	1933	1944	1940	A	1731	1735	1735
B	457	461	458	B	501	507	503
C	419	423	420	C	403	409	405
$\mu_a$	3.2	3.1	3.2	$\mu_a$	-0.1	0.1	0.1
$\mu_b$	-0.4	0.4	0.4	$\mu_b$	0.1	-0.1	-0.1
$\mu_c$	-0.6	0.6	0.6	$\mu_c$	-0.3	-0.3	-0.2
$\Delta E$	688	857	736	$\Delta E$	869	1117	902
$\Delta E_{ZPE}$	591	786	661	$\Delta E_{ZPE}$	693	956	744
$\Delta G_{298K}$	727	827	769	$\Delta G_{298K}$	721	884	746
TG+T/G-T/c	B3LYP-GD3BJ	MP2	B2PLYPD	G+G+T/G-G+/c	B3LYP-GD3BJ	MP2	B2PLYPD
A	1731	1731	1733	A	1381	1394	1387
B	499	505	501	B	610	616	612
C	403	408	405	C	502	514	505
$\mu_a$	-1.2	1.3	1.2	$\mu_a$	-0.6	-0.8	0.6
$\mu_b$	0.2	-0.3	-0.3	$\mu_b$	-1.2	1.4	-1.2
$\mu_c$	1.9	2.1	1.9	$\mu_c$	1.8	-1.7	-1.8
$\Delta E$	760	1097	833	$\Delta E$	636	761	679
$\Delta E_{ZPE}$	635	960	714	$\Delta E_{ZPE}$	585	709	639
$\Delta G_{298K}$	769	948	798	$\Delta G_{298K}$	768	772	751
G-TG-/G+T/c	B3LYP-GD3BJ	MP2	B2PLYPD	G-TG-/TT/cc	B3LYP-GD3BJ	MP2	B2PLYPD
A	1699	1656	1683	A	1810	1824	1819
B	514	525	518	B	462	467	463

C	493	505	498	C	441	447	443
$\mu_a$	-1.3	-1.7	1.5	$\mu_a$	0.0	0.0	0.0
$\mu_b$	-0.3	-0.4	0.4	$\mu_b$	0.5	0.5	0.5
$\mu_c$	-0.8	-0.5	-0.7	$\mu_c$	0.0	0.0	0.0
$\Delta E$	417	619	542	$\Delta E$	128	488	309
$\Delta E_{ZPE}$	420	516	515	$\Delta E_{ZPE}$	200	572	398
$\Delta G_{298K}$	657	511	680	$\Delta G_{298K}$	449	731	619
G-TG-/G-T/cc	B3LYP-GD3BJ	MP2	B2PLYPD	G-TG+/TG-/cc	B3LYP-GD3BJ	MP2	B2PLYPD
A	1422	1434	1429	A	1501	1501	1503
B	564	571	566	B	518	524	520
C	493	501	496	C	477	483	479
$\mu_a$	-2.7	2.7	2.8	$\mu_a$	5.0	-4.9	-4.9
$\mu_b$	-0.9	0.9	0.9	$\mu_b$	1.6	-1.5	-1.6
$\mu_c$	1.0	1.0	1.0	$\mu_c$	-0.5	-0.5	-0.5
$\Delta E$	269	453	369	$\Delta E$	594	904	704
$\Delta E_{ZPE}$	319	522	437	$\Delta E_{ZPE}$	571	822	674
$\Delta G_{298K}$	543	672	640	$\Delta G_{298K}$	798	918	859
G+TG-/G-T/cc	B3LYP-GD3BJ	MP2	B2PLYPD	G+G+G-/G+G+/c	B3LYP-GD3BJ	MP2	B2PLYPD
A	1582	1589	1587	A	1313	1329	1319
B	528	533	530	B	682	688	684
C	459	464	461	C	507	513	509
$\mu_a$	-1.7	-1.7	1.7	$\mu_a$	-0.8	0.8	0.8
$\mu_b$	2.3	2.3	-2.3	$\mu_b$	-0.5	-0.6	-0.5
$\mu_c$	0.5	0.5	0.5	$\mu_c$	-1.3	1.4	1.4
$\Delta E$	450	837	604	$\Delta E$	0	404	170
$\Delta E_{ZPE}$	456	826	618	$\Delta E_{ZPE}$	220	593	392
$\Delta G_{298K}$	704	949	827	$\Delta G_{298K}$	618	795	725
TG-G-/TG+/c	B3LYP-GD3BJ	MP2	B2PLYPD	G+G+T/G+T/c	B3LYP-GD3BJ	MP2	B2PLYPD
A	1261	1254	1259	A	1508	1519	1512
B	647	659	651	B	525	532	528
C	585	593	587	C	464	468	465
$\mu_a$	-2.8	-2.6	-2.7	$\mu_a$	-1.3	1.4	1.4
$\mu_b$	-0.3	-0.4	-0.4	$\mu_b$	0.4	-0.4	-0.4
$\mu_c$	-0.7	-0.8	-0.8	$\mu_c$	1.5	1.5	1.5
$\Delta E$	267	765	482	$\Delta E$	810	931	829
$\Delta E_{ZPE}$	333	737	522	$\Delta E_{ZPE}$	686	807	714
$\Delta G_{298K}$	690	908	817	$\Delta G_{298K}$	797	817	793
G-TG-/G-T/c	B3LYP-GD3BJ	MP2	B2PLYPD	G+TG+/TG-/cc	B3LYP-GD3BJ	MP2	B2PLYPD
A	1401	1407	1404	A	1597	1604	1601
B	560	569	563	B	528	536	531
C	485	493	487	C	443	448	445
$\mu_a$	-2.3	2.3	-2.3	$\mu_a$	4.4	-4.3	-4.3

$\mu_b$	0.2	-0.2	-0.2	$\mu_b$	1.2	-1.1	-1.2
$\mu_c$	-1.1	-1.0	1.0	$\mu_c$	1.9	1.9	1.9
$\Delta E$	649	840	749	$\Delta E$	712	961	804
$\Delta E_{ZPE}$	590	755	688	$\Delta E_{ZPE}$	679	911	774
$\Delta G_{298K}$	740	796	797	$\Delta G_{298K}$	923	1048	982
G+TG-/G-T/c	B3LYP-GD3BJ	MP2	B2PLYPD	G+TG+/TG+/cc	B3LYP-GD3BJ	MP2	B2PLYPD
A	1571	1576	1574	A	1701	1720	1710
B	527	532	528	B	515	521	517
C	458	463	460	C	473	476	474
$\mu_a$	-2.6	-2.6	-2.6	$\mu_a$	-3.1	-3.1	-3.1
$\mu_b$	-2.0	-2.1	-2.1	$\mu_b$	0.6	0.6	0.6
$\mu_c$	0.5	0.4	0.5	$\mu_c$	0.2	0.2	0.2
$\Delta E$	689	983	802	$\Delta E$	612	880	718
$\Delta E_{ZPE}$	633	948	764	$\Delta E_{ZPE}$	604	831	707
$\Delta G_{298K}$	825	1016	915	$\Delta G_{298K}$	877	1001	947
G+TG-/G-G-/cc	B3LYP-GD3BJ	MP2	B2PLYPD	G-TG-/G-T/cc	B3LYP-GD3BJ	MP2	B2PLYPD
A	1302	1307	1305	A	1418	1431	1425
B	600	608	603	B	560	568	563
C	537	545	540	C	490	499	493
$\mu_a$	-1.1	1.1	1.1	$\mu_a$	-2.6	2.7	-2.7
$\mu_b$	3.6	3.6	3.6	$\mu_b$	-0.2	0.2	0.2
$\mu_c$	-0.8	0.8	0.8	$\mu_c$	-0.9	-0.9	0.9
$\Delta E$	738	975	821	$\Delta E$	379	680	528
$\Delta E_{ZPE}$	696	918	788	$\Delta E_{ZPE}$	428	719	583
$\Delta G_{298K}$	908	1018	966	$\Delta G_{298K}$	633	838	761
TTG-/TT/c	B3LYP-GD3BJ	MP2	B2PLYPD	TG-G-/TG+/c	B3LYP-GD3BJ	MP2	B2PLYPD
A	1860	1858	1862	A	1266	1258	1264
B	443	447	444	B	641	653	645
C	416	422	418	C	579	587	582
$\mu_a$	2.0	1.9	2.0	$\mu_a$	-1.1	-0.8	-1.0
$\mu_b$	1.1	1.3	1.2	$\mu_b$	-1.2	-1.2	-1.2
$\mu_c$	0.9	0.9	0.9	$\mu_c$	-1.9	-1.9	-1.9
$\Delta E$	1159	1193	1158	$\Delta E$	330	920	584
$\Delta E_{ZPE}$	965	1010	976	$\Delta E_{ZPE}$	417	899	639
$\Delta G_{298K}$	985	951	968	$\Delta G_{298K}$	778	1057	933
G+TG+/G-G+/cc	B3LYP-GD3BJ	MP2	B2PLYPD	G+G+T/G+G+/cc	B3LYP-GD3BJ	MP2	B2PLYPD
A	1419	1433	1425	A	1492	1499	1494
B	615	623	618	B	549	558	553
C	530	532	530	C	501	508	503
$\mu_a$	-2.3	2.4	2.4	$\mu_a$	0.9	-0.8	-0.9
$\mu_b$	3.0	-3.1	-3.0	$\mu_b$	-0.4	0.5	0.4
$\mu_c$	-0.8	-0.7	-0.8	$\mu_c$	0.5	0.5	0.5

$\Delta E$	357	854	571	$\Delta E$	686	848	760
$\Delta E_{ZPE}$	448	853	639	$\Delta E_{ZPE}$	658	809	736
$\Delta G_{298K}$	844	1099	983	$\Delta G_{298K}$	731	830	795
G-TG-/G+T/cc	B3LYP-GD3BJ	MP2	B2PLYPD	G+TG-/G-G+/cc	B3LYP-GD3BJ	MP2	B2PLYPD
A	1557	1583	1568	A	1389	1402	1395
B	533	536	534	B	623	630	625
C	502	508	504	C	515	521	517
$\mu_a$	-1.9	-1.9	1.9	$\mu_a$	-0.3	0.4	0.4
$\mu_b$	0.6	0.6	-0.6	$\mu_b$	1.5	1.4	1.4
$\mu_c$	-1.0	-1.1	-1.0	$\mu_c$	-0.1	0.0	0.0
$\Delta E$	363	795	887	$\Delta E$	758	1181	928
$\Delta E_{ZPE}$	409	837	940	$\Delta E_{ZPE}$	699	1083	866
$\Delta G_{298K}$	666	1003	1165	$\Delta G_{298K}$	904	1172	1036
G+TG+/G+G-/c	B3LYP-GD3BJ	MP2	B2PLYPD	G-G+T/G+G-/c	B3LYP-GD3BJ	MP2	B2PLYPD
A	1526	1535	1531	A	1240	1230	1236
B	547	553	549	B	690	707	696
C	497	502	499	C	523	537	528
$\mu_a$	-3.0	-3.0	-3.0	$\mu_a$	2.1	2.0	2.1
$\mu_b$	-1.3	1.3	1.3	$\mu_b$	-0.9	-1.0	-1.0
$\mu_c$	-0.3	0.3	0.3	$\mu_c$	1.7	1.8	1.7
$\Delta E$	549	1073	756	$\Delta E$	628	1003	765
$\Delta E_{ZPE}$	592	1045	785	$\Delta E_{ZPE}$	662	1043	815
$\Delta G_{298K}$	852	1150	992	$\Delta G_{298K}$	938	1181	1048
G+TG+/G+G-/c	B3LYP-GD3BJ	MP2	B2PLYPD	TG+G-/TG+/cc	B3LYP-GD3BJ	MP2	B2PLYPD
A	1531	1540	1537	A	1278	1286	1281
B	548	555	550	B	647	653	649
C	498	503	499	C	481	487	483
$\mu_a$	-3.5	-3.5	-3.5	$\mu_a$	2.5	2.4	2.4
$\mu_b$	-1.9	1.9	1.9	$\mu_b$	-0.8	-0.9	-0.9
$\mu_c$	1.3	-1.4	-1.3	$\mu_c$	-0.2	-0.1	-0.2
$\Delta E$	610	1054	778	$\Delta E$	597	1083	755
$\Delta E_{ZPE}$	646	1041	810	$\Delta E_{ZPE}$	657	1093	811
$\Delta G_{298K}$	890	1140	1006	$\Delta G_{298K}$	892	1192	1002
G+TG+/G+G+/c	B3LYP-GD3BJ	MP2	B2PLYPD	G-TG-/G+G+/cc	B3LYP-GD3BJ	MP2	B2PLYPD
A	1436	1452	1444	A	1386	1421	1400
B	616	624	619	B	605	606	605
C	521	525	522	C	584	592	587
$\mu_a$	-1.6	1.5	1.5	$\mu_a$	0.0	0.0	0.0
$\mu_b$	-2.1	2.1	2.1	$\mu_b$	-0.2	0.4	0.3
$\mu_c$	0.6	0.4	0.5	$\mu_c$	0.0	0.0	0.0
$\Delta E$	657	972	808	$\Delta E$	536	1028	768
$\Delta E_{ZPE}$	613	947	786	$\Delta E_{ZPE}$	574	1039	803

$\Delta G_{298K}$	829	1134	1015	$\Delta G_{298K}$	848	1220	1045
G-TG-/G+T/cc	B3LYP-GD3BJ	MP2	B2PLYPD	G-TG-/G+G-/cc	B3LYP-GD3BJ	MP2	B2PLYPD
A	1747	1740	1747	A	1397	1390	1396
B	510	515	512	B	591	606	596
C	485	493	487	C	567	575	570
$\mu_a$	-1.0	-1.0	-1.0	$\mu_a$	2.1	-2.1	-2.1
$\mu_b$	0.4	0.4	0.4	$\mu_b$	-1.3	1.4	1.4
$\mu_c$	-1.2	-1.2	-1.3	$\mu_c$	-2.1	-2.1	-2.1
$\Delta E$	292	987	605	$\Delta E$	449	963	680
$\Delta E_{ZPE}$	461	1073	760	$\Delta E_{ZPE}$	590	1021	805
$\Delta G_{298K}$	806	1266	1053	$\Delta G_{298K}$	908	1206	1078
G-TG-/G+G-/cc'	B3LYP-GD3BJ	MP2	B2PLYPD	G-G-G-/TG+/c	B3LYP-GD3BJ	MP2	B2PLYPD
A	1394	1388	1394	A	1206	1236	1214
B	586	601	591	B	700	696	699
C	563	572	566	C	656	650	655
$\mu_a$	1.7	-1.8	-1.8	$\mu_a$	-2.2	-1.8	-2.1
$\mu_b$	-1.4	1.4	1.4	$\mu_b$	-1.1	1.1	1.1
$\mu_c$	-0.1	-0.2	-0.1	$\mu_c$	2.0	-2.2	-2.0
$\Delta E$	533	1159	812	$\Delta E$	424	1304	821
$\Delta E_{ZPE}$	677	1204	933	$\Delta E_{ZPE}$	629	1383	991
$\Delta G_{298K}$	980	1367	1188	$\Delta G_{298K}$	1098	1581	1373

**Table S02.** Cartesian coordinates in Angstroms (Å) of detected conformers f mannitol at B2PLYP-GD3BJ/6-311++G (d,p) level of theory.

TG+T/G+T/c				TG+T/G+G+/c				TG-T/TT/c			
Atom	X	Y	Z	Atom	X	Y	Z	Atom	X	Y	Z
C	-1.496	-0.612	0.482	C	1.626	-0.131	-0.240	C	1.509	-0.031	-0.231
C	-0.761	0.583	-0.162	C	0.594	0.856	0.295	C	0.713	0.295	1.035
C	0.742	0.637	0.126	C	-0.849	0.580	-0.146	C	-0.713	-0.294	1.035
C	1.552	-0.478	-0.548	C	-1.492	-0.681	0.474	C	-1.509	0.031	-0.231
C	3.045	-0.181	-0.557	C	-3.005	-0.558	0.546	C	-2.964	-0.377	-0.103
O	3.537	-0.059	0.780	O	-3.560	-0.126	-0.700	O	-3.602	0.073	-1.307
O	1.316	-1.728	0.113	O	-1.219	-1.822	-0.334	O	-1.423	1.444	-0.458
O	1.275	1.872	-0.342	O	-1.561	1.771	0.217	O	-0.707	-1.699	1.252
O	-1.268	1.834	0.323	O	1.000	2.131	-0.189	O	0.707	1.699	1.252
O	-1.383	-1.767	-0.341	O	1.383	-1.417	0.341	O	1.423	-1.444	-0.458
C	-2.983	-0.330	0.640	C	3.041	0.307	0.101	C	2.964	0.377	-0.103
O	-3.556	0.191	-0.561	O	3.883	-0.787	-0.292	O	3.602	-0.073	-1.307
H	-1.084	-0.808	1.480	H	1.531	-0.196	-1.331	H	1.072	0.503	-1.083
H	-0.910	0.524	-1.246	H	0.629	0.840	1.394	H	1.226	-0.150	1.892
H	0.883	0.563	1.214	H	-0.866	0.463	-1.235	H	-1.226	0.150	1.892
H	1.211	-0.609	-1.578	H	-1.113	-0.834	1.492	H	-1.072	-0.503	-1.083
H	3.566	-1.030	-1.000	H	-3.419	-1.526	0.843	H	-3.038	-1.461	0.009
H	3.250	0.716	-1.141	H	-3.293	0.191	1.282	H	-3.404	0.116	0.771
H	3.362	0.842	1.070	H	-3.326	-0.789	-1.357	H	-4.550	-0.049	-1.222
H	1.865	-1.733	0.908	H	-0.272	-2.006	-0.232	H	-2.096	1.663	-1.113
H	0.597	2.535	-0.151	H	-2.399	1.745	-0.260	H	-0.050	-2.067	0.646
H	-2.134	1.958	-0.083	H	0.223	2.698	-0.101	H	0.050	2.068	0.645
H	-0.479	-2.100	-0.235	H	2.202	-1.917	0.224	H	2.096	-1.663	-1.113
H	-3.481	-1.255	0.943	H	3.291	1.220	-0.441	H	3.038	1.461	0.009
H	-3.148	0.425	1.406	H	3.119	0.484	1.180	H	3.404	-0.116	0.771
H	-3.456	-0.483	-1.242	H	4.778	-0.619	0.014	H	4.550	0.049	-1.222

Figure S02. 50 lowest-energy structures of mannitol.

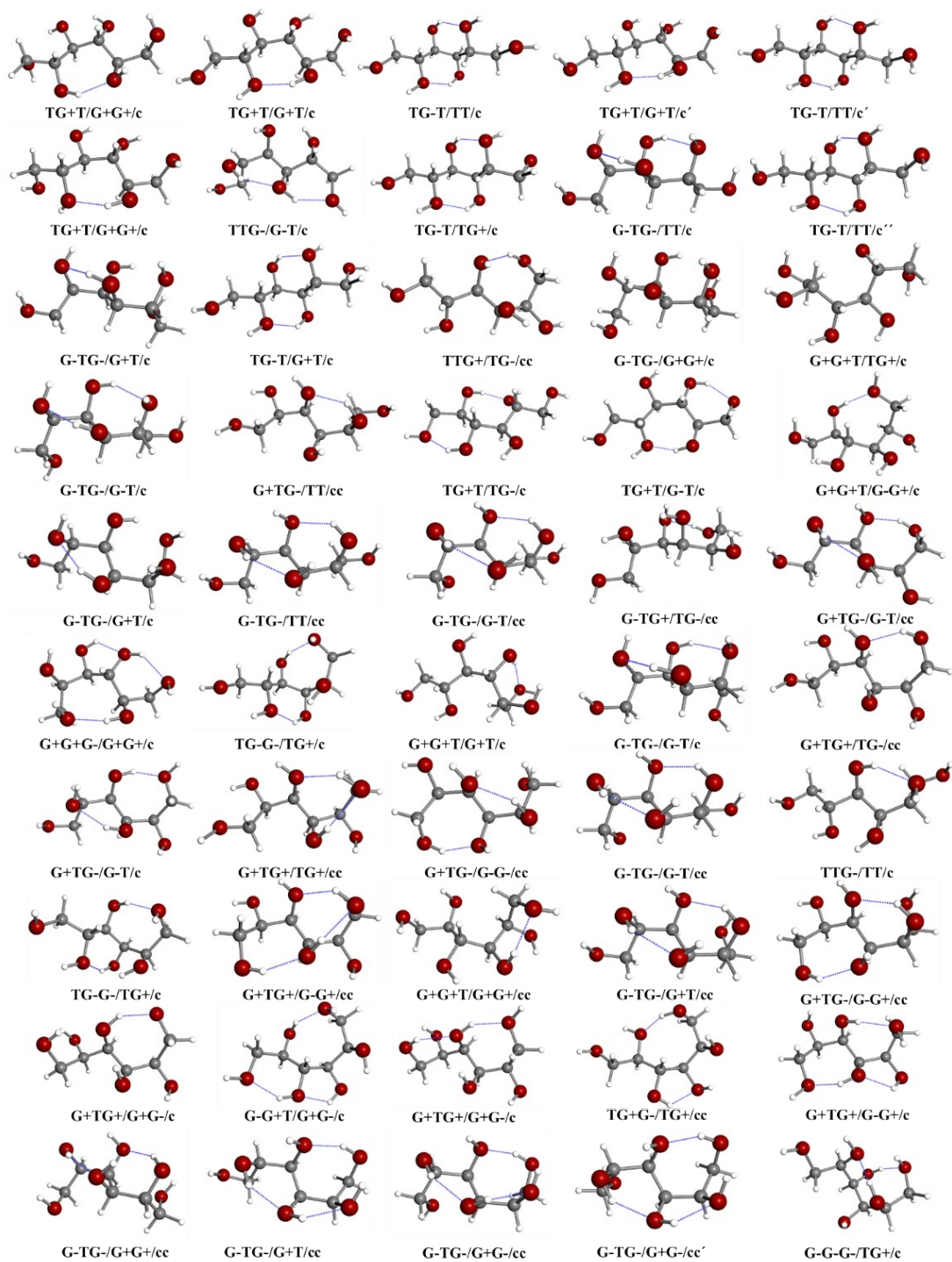


**Figure S03.** Summary of reaction network of fragment species of mannitol predicted by Automekin. Blue arrows represent barrierless processes, while black arrows indicate reactions with an energetic barrier.

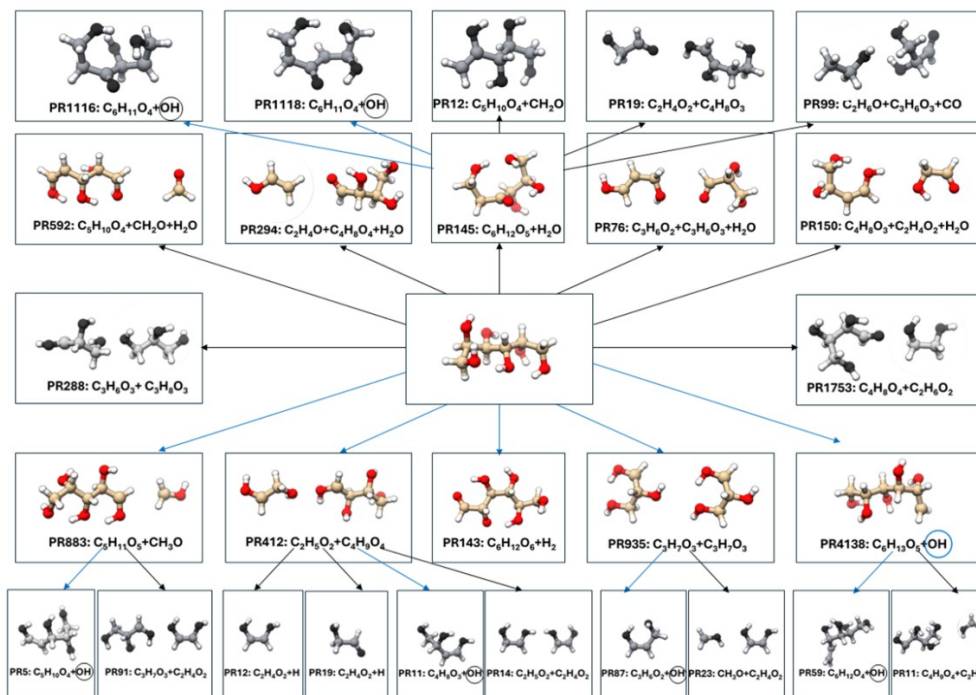


**Table S03.** Summary of known molecular species detected in the broadband spectrum of laser ablated mannitol.

Name	Formula	$N^a$
Formaldehyde	COH <sub>2</sub>	1
Hydroxy Radical	OH	2
Acetic Acid	C <sub>2</sub> O <sub>2</sub> H <sub>4</sub>	4
Ethylene glycol (aGg' conformer)	C <sub>2</sub> O <sub>2</sub> H <sub>6</sub>	5
Glycolic Acid	C <sub>2</sub> O <sub>3</sub> H <sub>4</sub>	2
Syn-vinyl alcohol	C <sub>2</sub> OH <sub>4</sub>	1
Anti-vinyl alcohol	C <sub>2</sub> OH <sub>4</sub>	1
Acetaldehyde	C <sub>2</sub> OH <sub>4</sub>	7
Ethanol	C <sub>2</sub> OH <sub>6</sub>	1
Oxopropadienylidene	C <sub>3</sub> O	1
Malonaldehyde	C <sub>3</sub> O <sub>2</sub> H <sub>4</sub>	2
2-Hydroxypropenal	C <sub>3</sub> O <sub>2</sub> H <sub>4</sub>	5
2-Hydroxypropanal	C <sub>3</sub> O <sub>2</sub> H <sub>6</sub>	3
3-Hydroxypropanal	C <sub>3</sub> O <sub>2</sub> H <sub>6</sub>	3
Glyceraldehyde (E conformers)	C <sub>3</sub> O <sub>3</sub> H <sub>5</sub>	9
Glycolaldehyde	C <sub>3</sub> O <sub>3</sub> H <sub>6</sub>	2
Glycerol (G'Gg'gg' conformer)	C <sub>3</sub> O <sub>3</sub> H <sub>8</sub>	2
Glycerol (GGag'g' conformer)	C <sub>3</sub> O <sub>3</sub> H <sub>8</sub>	4
Propynal	C <sub>3</sub> OH <sub>2</sub>	1
Trans-propenal/ Acrolein	C <sub>3</sub> OH <sub>4</sub>	1
Syn-Propanal	C <sub>3</sub> OH <sub>6</sub>	4
1-Butyne	C <sub>4</sub> H <sub>5</sub>	1
1,3-Pentadiyne	C <sub>5</sub> H <sub>4</sub>	2

<sup>a</sup> $N$  represents the number of observed rotational transitions. <sup>b</sup>Species assigned with a single detected transition are classified as tentative. However, their assignment is robustly supported as the observed lines correspond to their most intense expected transitions under jet-cooled conditions, they are predicted as photofragments by AutoMeKin, and they are commonly observed ablation products in related molecules.

**Table S04.** Measured rotational transitions of Rotamer I (TG+T/G+G+/c).

J'	K' <sub>a</sub>	K' <sub>c</sub>	J''	K'' <sub>a</sub>	K'' <sub>c</sub>	V <sub>obs</sub>	V <sub>obs</sub> -V <sub>cal</sub>
3	2	1	2	2	0	2843.245	-0.002
4	0	4	3	0	3	3699.351	-0.011
4	2	2	3	2	1	3813.510	0.034
4	1	3	3	1	2	3942.986	0.002
5	1	5	4	1	4	4427.928	0.031
5	0	5	4	0	4	4583.369	0.012
5	2	4	4	2	3	4684.998	0.013
5	2	3	4	2	2	4800.063	0.010
6	1	6	5	1	5	5300.138	0.014
6	0	6	5	0	5	5447.027	0.018
6	2	5	5	2	4	5610.922	0.014
6	3	4	5	3	3	5665.415	0.014
6	3	3	5	3	2	5678.317	-0.005
6	2	4	5	2	3	5801.828	0.016
6	1	5	5	1	4	5878.457	0.015
7	1	7	6	1	6	6166.833	0.014
7	1	7	6	1	6	6166.835	0.016
3	2	1	2	1	1	6292.131	0.037
7	0	7	6	0	6	6294.113	0.012
7	2	6	6	2	5	6530.938	0.015
3	2	2	2	1	2	6557.484	0.002
7	6	1	6	6	0	6594.944	0.019
7	6	2	6	6	1	6594.944	0.019
7	5	3	6	5	2	6599.508	0.019
7	5	2	6	5	1	6599.508	0.019
7	4	4	6	4	3	6607.811	0.021
7	4	3	6	4	2	6608.714	0.029
7	3	5	6	3	4	6614.766	0.014
7	3	4	6	3	3	6643.371	0.014
5	1	4	4	0	4	6678.142	0.023
7	2	5	6	2	4	6813.824	0.019
7	1	6	6	1	5	6827.997	0.014
8	1	8	7	1	7	7028.270	0.015
8	0	8	7	0	7	7130.652	0.009
4	2	2	3	1	2	7142.605	0.015
8	2	7	7	2	6	7444.233	0.010
8	7	1	7	7	0	7536.523	0.007
8	7	2	7	7	1	7536.523	0.007
8	6	3	7	6	2	7540.555	0.017
8	6	2	7	6	1	7540.555	0.017

8	5	4	7	5	3	7547.373	0.011
8	5	3	7	5	2	7547.373	0.011
8	4	5	7	4	4	7559.286	0.015
8	4	4	7	4	3	7561.728	0.016
8	3	6	7	3	5	7564.051	0.015
8	3	5	7	3	4	7619.816	0.016
4	2	3	3	1	3	7643.952	0.006
8	1	7	7	1	6	7760.775	0.010
8	2	6	7	2	5	7828.720	0.006
9	1	9	8	1	8	7884.990	0.015
9	0	9	8	0	8	7962.474	0.009
6	1	5	5	0	5	7973.226	0.022
5	2	3	4	1	3	7999.664	0.004
9	2	8	8	2	7	8350.165	0.005
9	7	2	8	7	1	8481.837	0.021
9	7	3	8	7	2	8481.837	0.021
9	6	4	8	6	3	8487.564	0.013
9	6	3	8	6	2	8487.564	0.013
9	5	5	8	5	4	8497.274	-0.016
9	5	4	8	5	3	8497.274	-0.016
9	3	7	8	3	6	8511.954	-0.003
9	4	6	8	4	5	8513.245	0.007
9	4	5	8	4	4	8519.057	0.023
9	3	6	8	3	5	8610.311	0.003
9	1	8	8	1	7	8673.336	0.004
10	1	10	9	1	9	8737.696	0.005
5	2	4	4	1	4	8778.669	-0.035
10	0	10	9	0	9	8793.590	-0.003
3	3	0	2	2	0	8801.232	-0.006
3	3	1	2	2	1	8807.063	-0.017
9	2	7	8	2	6	8839.176	0.005
6	2	4	5	1	4	8885.759	-0.007
10	2	9	9	2	8	9248.296	0.005
10	7	4	9	7	3	9428.266	0.005
10	7	3	9	7	2	9428.266	0.005
10	6	5	9	6	4	9436.142	0.003
10	6	4	9	6	3	9436.142	0.003
10	5	6	9	5	5	9449.340	0.003
10	5	5	9	5	4	9449.767	0.002
10	3	8	9	3	7	9457.061	-0.002
10	4	7	9	4	6	9469.520	-0.003
10	4	6	9	4	5	9481.890	0.000
10	1	9	9	1	8	9563.222	-0.005
11	1	11	10	1	10	9587.161	-0.007
10	3	7	9	3	6	9616.493	-0.008
11	0	11	10	0	10	9626.048	0.008

4	3	1	3	2	1	9729.665	0.001
4	3	2	3	2	2	9758.256	-0.001
10	2	8	9	2	7	9839.284	-0.010
6	2	5	5	1	5	9961.715	0.000
11	2	10	10	2	9	10138.412	-0.012
11	8	3	10	8	2	10369.286	0.017
11	8	4	10	8	3	10369.286	0.017
11	7	5	10	7	4	10376.002	0.019
11	7	4	10	7	3	10376.002	0.019
11	6	6	10	6	5	10386.479	-0.013
11	6	5	10	6	4	10386.479	-0.013
11	3	9	10	3	8	10397.858	-0.022
11	5	7	10	5	6	10403.896	-0.011
11	5	6	10	5	5	10404.956	-0.014
11	4	8	10	4	7	10427.668	-0.030
11	1	10	10	1	9	10430.152	-0.021
12	1	12	11	1	11	10434.132	-0.009
11	4	7	10	4	6	10451.900	-0.010
12	0	12	11	0	11	10460.416	-0.006
11	3	8	10	3	7	10637.740	-0.016
5	3	3	4	2	3	10721.221	0.006
11	2	9	10	2	8	10824.773	-0.039
12	2	11	11	2	10	11020.652	0.002
12	1	11	11	1	10	11276.875	-0.018
13	1	13	12	1	12	11279.235	-0.017
13	0	13	12	0	12	11296.612	-0.026
12	3	10	11	3	9	11332.980	-0.035
12	5	8	11	5	7	11361.042	-0.026
12	5	7	11	5	6	11363.479	0.009
12	4	9	11	4	8	11387.022	-0.028
12	4	8	11	4	7	11431.130	-0.024
12	2	10	11	2	9	11792.368	-0.048

---

**Table S05.** Measured rotational transitions of Rotamer II (TG+T/G+T/c).

J'	K' <sub>a</sub>	K' <sub>c</sub>	J''	K'' <sub>a</sub>	K'' <sub>c</sub>	V <sub>obs</sub>	V <sub>obs</sub> -V <sub>cal</sub>
3	2	1	2	1	1	6387.635	0.016
3	2	1	2	1	2	6668.402	0.029
7	1	7	6	0	6	7010.973	0.005
4	2	3	3	1	2	7206.527	-0.008
4	2	2	3	1	2	7288.733	0.014
8	1	8	7	0	7	7799.109	0.002
5	2	4	4	1	3	8006.491	-0.017
3	3	1	2	2	0	8856.184	-0.011
3	3	0	2	2	0	8856.401	0.000
3	3	0	2	2	1	8861.955	-0.011
11	1	10	10	2	9	9573.531	-0.006
4	3	2	3	2	1	9832.342	0.013
4	3	1	3	2	1	9833.777	0.000
4	3	2	3	2	2	9859.997	-0.025
4	3	1	3	2	2	9861.462	-0.008
5	3	2	4	2	3	10874.911	0.018

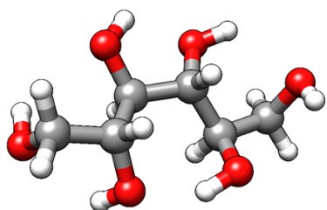
**Table S06.** Measured rotational transitions of Rotamer III (TG-T/TT/c).

J'	K' <sub>a</sub>	K' <sub>c</sub>	J''	K'' <sub>a</sub>	K'' <sub>c</sub>	V <sub>obs</sub>	V <sub>obs</sub> -V <sub>cal</sub>
4	2	2	3	1	2	6860.239	-0.010
4	2	3	3	1	3	6937.656	0.011
6	1	5	5	0	5	6954.435	-0.011
5	2	3	4	1	3	7803.595	0.004
5	2	4	4	1	4	7931.313	0.029
3	3	0	2	2	0	7950.197	0.008
3	3	1	2	2	1	7950.197	0.008
7	1	6	6	0	6	7970.718	-0.012
4	3	1	3	2	1	8917.100	0.010
4	3	2	3	2	2	8917.734	0.000
6	2	5	5	1	5	8931.539	-0.002
7	2	5	6	1	5	9677.097	-0.016
5	3	2	4	2	2	9883.552	-0.019
5	3	3	4	2	3	9885.500	0.004
6	3	3	5	2	3	10849.256	0.032
6	3	4	5	2	4	10853.711	0.012
4	4	0	3	3	0	10936.780	-0.037
4	4	1	3	3	1	10936.780	-0.037

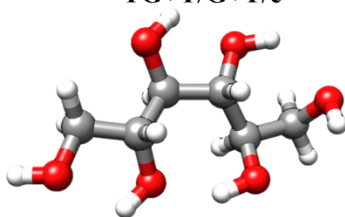
**Figure S04.** Comparison of gas phases conformations and crystal phase structure.

**Gas Phase**

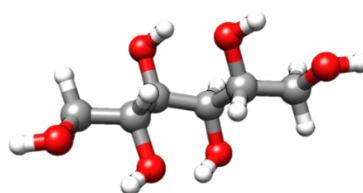
**TG+T/G+G+/c**



**TG+T/G+T/c**



**TG-T/TT/c**



**Crystal Phase**

*TTT/G+G+/c*

